ISSN 1063-7826, Semiconductors, 2015, Vol. 49, No. 13, pp. 1679–1683. © Pleiades Publishing, Ltd., 2015.
Original Russian Text © G.D. Demin, A.F. Popkov, N.A. Dyuzhev, 2015, published in Izvestiya vysshikh uchebnykh zavedenii. Elektronika, 2014, Vol. 108, No. 4, pp. 3–10.

BASIC RESEARCH

Spin-Transfer Torque and Specific Features of Magnetic-State Switching in Vacuum Tunnel Nanostructures

G. D. Demin, A. F. Popkov, and N. A. Dyuzhev

National Research University of Electronic Technology "MIET", Zelenograd, Moscow, 124498 Russia

e-mail: gddemin@gmail.com

Submitted December 12, 2013

Abstract—The specific features of spin-transfer torque in vacuum tunnel structures with magnetic electrodes are investigated using the quasi-classical Sommerfeld model of electron conductivity, which takes into account the exchange splitting of the spin energy subbands of free electrons. Using the calculated voltage dependences of the transferred torques for a tunnel structure with cobalt electrodes and noncollinear magnetic moments in the electrodes, diagrams of stable spin states on the current–field parameter plane in the in-plane geometry of the initial magnetization are obtained.

Keywords: spin torque, vacuum gap, spin-polarized electron emission, magnetic tunnel junction, spin state switching.

DOI: 10.1134/S1063782615130059

At present, tunnel spin-valve structures are being intensively studied as promising materials for application in new solid-state nonvolatile memory cells and nanoscale microwave generators [1–3]. Tunneling spacers are formed from MgO insulators, which enhance the spin-dependent tunneling and polarization of a passing current. To achieve a large value of this effect, it is important to form high-quality interfaces of the dielectric spacers, since the features of spin-torque tunnel transfer greatly depend on crystal-structure matching and homogeneity of the transition layers between the insulator and magnetic electrodes.

Investigation of the specific features of tunnel structures with a dielectric barrier is complicated by spin-dependent scattering at interlayer interfaces [4] and the possible formation of additional tunneling channels caused by impurities and defects in the dielectric layer [5]. In addition, such tunnel structures are limited by a breakdown voltage, which, in turn, restricts the transmitted current. Moreover, the densities of field-emission currents transmitted without destroying the electrodes overlap the range of threshold spin-state-switching current densities in magnetic tunnel structures (10^6–10^8 A/cm^2) and it is not necessary to match layers at the magnetic-electrode boundaries. Therefore, tunnel structures with a vacuum gap are interesting for studying the main features of the I–V characteristics and spin-switching thresholds. In a vacuum structure, higher voltages can be applied, which leads to new features of spin-transfer torque.

Original high-vacuum scanning tunneling microscopy experimental results on the magnetization switching of magnetic nanoislands by a spin-polarized current and the field features of the tunneling magnetoresistance were reported in [6, 7]. In addition, thermal-assisted magnetic recording based on spin-transfer torque in vacuum structures is considered to be an alternative method for creating a new generation of disc storage devices [8].

In this study, we analyze the spin-transport effects in structures with a vacuum gap in the tunnel and field-emission modes.

INITIAL EQUATIONS OF MACROSPIN MAGNETODYNAMICS

We investigate a vacuum tunnel structure consisting of a thick hard magnetic electrode with fixed magnetization $\mathbf{M}_p$ and a thin-film soft magnetic electrode with unfixed magnetization $\mathbf{M}$, which are separated by a tunneling spacer (insert in Fig. 1).

Let us consider the in-plane geometry of the magnetization of this structure. In a vacuum structure, the hard-magnetic electrode serves as a spin polarizer of the incoming current and set the spin direction of electrons tunneling through the vacuum gap. As a result of tunnel spin-torque transfer to the thin-film electrode by conduction electrons, the magnetization vector $\mathbf{m} = \mathbf{M}/M_S$, where M_S is the saturation magnetization, can lose its stability. This ultimately leads to switching of the soft-magnetic layer. To analyze the stability of the magnetic state in the vacuum tunnel structure, we will use the Landau–Lifshitz equation

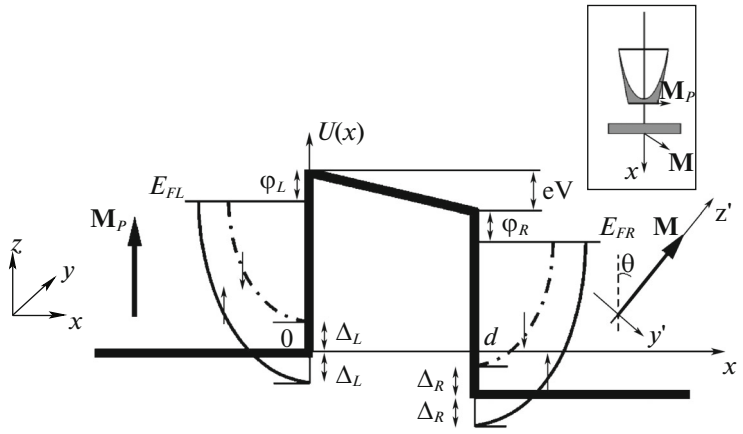

Fig. 1. Schematic of the potential-barrier shape for the vacuum tunnel structure in the transverse direction (along the *OX* axis): $E_{FL}(E_{FR})$ is the Fermi level (chemical potential) for the left (right) magnetic layer, $\Delta_L(\Delta_R)$ is the exchange splitting in the left (right) magnetic layer, $\varphi_L(\varphi_R)$ is the electron work function for the left (right) magnetic layer, V is the applied voltage, and d is the tunnel barrier thickness. The insert shows a cross section of the vacuum tunnel structure with in-plane magnetization geometry.

generalized by Slonczewski with Gilbert damping in the presence of both spin-torque components

$$\frac{\partial \mathbf{m}}{\partial t} = -\gamma_0 \cdot \mathbf{m} \times \mathbf{H}_{EFF} + \alpha\left(\mathbf{m} \times \frac{\partial \mathbf{m}}{\partial t}\right) - \frac{\gamma}{M_S d_F}(\mathbf{T}_\parallel + \mathbf{T}_\perp), \quad (1)$$

where $\gamma_0 = \mu_0\gamma$; μ_0 is the magnetic constant; γ is the gyromagnetic ratio; α is the Gilbert damping coefficient; d_F is the thickness of the unfixed soft-magnetic layer; $\mathbf{H}_{EFF} = \mathbf{H} + \mathbf{H}_K + \mathbf{H}_D$ is the effective magnetic field including external magnetic field $\mathbf{H}$, anisotropy field $\mathbf{H}_K$, and demagnetizing field $\mathbf{H}_D$; and $\mathbf{T}_\parallel$ and $\mathbf{T}_\perp$ are the parallel and perpendicular spin-torque components, respectively.

Components $\mathbf{T}_\parallel$ and $\mathbf{T}_\perp$ of the transferred torque can be presented in the form

$$\mathbf{T}_\parallel = \frac{\hbar J}{2e}\eta_\parallel[\mathbf{m} \times [\mathbf{m} \times \mathbf{m}_P]],$$

$$\mathbf{T}_\perp = \frac{\hbar J}{2e}\eta_\perp[\mathbf{m} \times \mathbf{m}_P],$$

where $\hbar$ is Planck's constant, J is the current density, e is the electron charge, $\mathbf{m}_P$ is the normalized vector of magnetization of the polarizer layer, and $\eta_\parallel$ and $\eta_\perp$ are the spin efficiency parameters depending on the mutual orientation of vectors $\mathbf{m}$ and $\mathbf{m}_P$.

SPIN TORQUE

The transferred torque $\mathbf{T}$ will be calculated using the thermodynamically averaged quantum-mechanical expression for the density of the total spin flow between semi-infinite magnetic electrodes

$$\mathbf{T} = \mathbf{T}_\parallel + \mathbf{T}_\perp = \frac{\hbar}{2}\left(\left\langle \mathbf{J}_S^{L\to R}\right\rangle - \left\langle \mathbf{J}_S^{R\to L}\right\rangle\right). \quad (2)$$

Here, $\left\langle \mathbf{J}_S^{L\to R}\right\rangle$ and $\left\langle \mathbf{J}_S^{R\to L}\right\rangle$ are the spin flow of electrons tunneling from the left to the right and from the right to the left, respectively, thermodynamically averaged with regard to the energy density of free electrons in the magnetic electrodes on the basis of the Fermi distribution

$$f(E) = [\exp(E - E_F)/k_BT + 1]^{-1},$$

where E is the electron energy, E_F is the Fermi energy in the corresponding electrode, k_B is the Boltzmann constant, and T is the temperature.

The angular brackets in (2) indicate the quantum-mechanical and thermodynamic averaging in the phase space of wave numbers of tunneling electrons.

According to the quantum-mechanical definition, spin-flow components $J_{\mu S}$ for tunneling electrons, where $\mu = x, y, z$, are calculated using the formula

$$J_{\mu S} = \frac{i\hbar}{2m^*}\sum_S\left(\Psi^{S*}\hat{\sigma}_\mu\Psi^S - \Psi^{S*}\hat{\sigma}_\mu\Psi^S\right),$$

where m^* is the effective mass, $S = \pm 1/2$ is the electron spin projection, Ψ^{S*} is the conjugate component of the spinor wavefunction, $\hat{\sigma}_\mu$ is the corresponding Pauli matrix, and Ψ^S is the spinor wavefunction of tunneling electrons.

Wavefunction Ψ^S is determined by solving the quantum-mechanical problem of electron tunneling across a tunnel structure for the potential shown in Fig. 1. This potential makes allowance for the energy barrier related to the work function and voltage drop at the vacuum gap. In the calculation of the spin flow, we shall restrict our consideration to the low-temperature

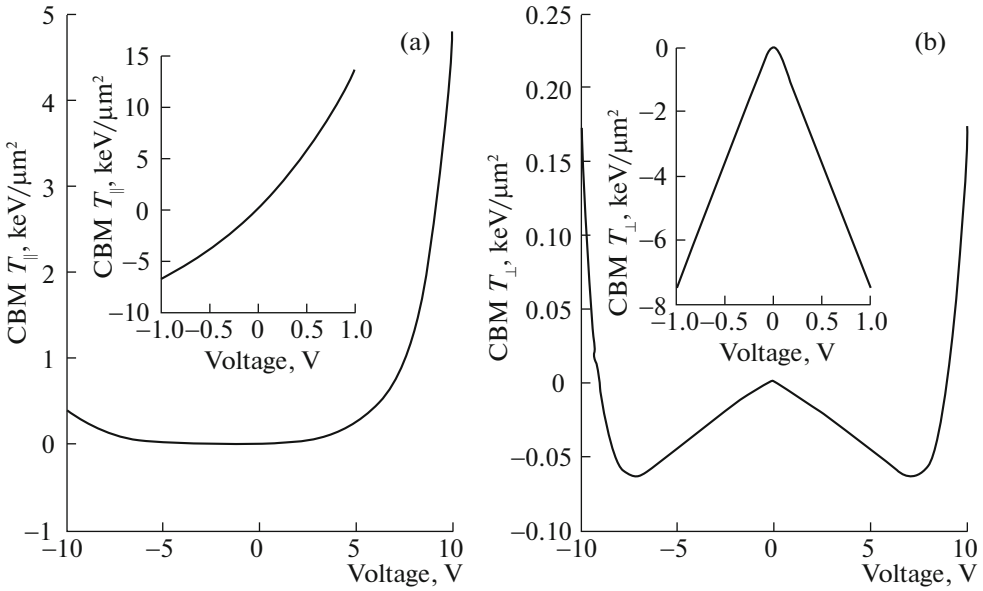

Fig. 2. Dependence of torques (a) $T_{\parallel}$ and (b) $T_{\perp}$ transferred by the spin current on voltage V. The insert shows the region from −1 to +1 V.

limit of the Fermi-energy distribution for conduction electrons and use the expression for the density of states, as in the free electron model, but with regard to the exchange splitting of the spin subbands.

According to Slonczewski theory for a magnetic tunnel junction [9], the spin efficiency parameters $\eta_{\parallel}$ and $\eta_{\perp}$ in the limit $V \to 0$ are determined by the bulk spin polarization P as

$$\eta_{\parallel} = \frac{P}{1 + P^2 \cos\theta}, \quad \eta_{\perp} = -\beta\eta_{\parallel}\mathrm{sgn}(J), \qquad (3)$$

where θ is the angle between vectors $\mathbf{m}$ and $\mathbf{m}_P$ and β is the coefficient of the proportionality of the spin-efficiency parameters.

Parameters $\eta_{\parallel}$ and $\eta_{\perp}$ are independent of the voltage applied to the structure and, consequently, of the flowing current. However, calculation of the spin flow shows that with increasing voltage these parameters significantly change, which greatly affects the regions of stability of spin states in vacuum tunnel structure and their switching thresholds.

To calculate the voltage dependence of the transferred spin-torque components, we use parameters corresponding to the Co(Fe)–vacuum–Co(Fe) structure [10], i.e., the Fermi level $E_{FL} = E_{FR} = 2.62$ eV, exchange splitting in ferromagnetic electrodes $\Delta_L = \Delta_R = 2.2$ eV, work function $\varphi_L = \varphi_R = 5.0$ eV, and the thickness of vacuum gap $d = 0.45$ nm.

Solving the quantum-mechanical problem of electron tunneling through the vacuum spacer and subsequent thermodynamic averaging of the charge and spin flows lead to the dependences of the spin-torque components on the bias voltage (Fig. 2). Calculation was performed for the mutually perpendicular orientation of vectors $\mathbf{m}$ and $\mathbf{m}_P$ in the ferromagnetic layers of structure.

The results obtained show the presence of highly nonmonotonic areas related to different tunneling modes in the low- and high-voltage regions with asymmetric sign variation. The latter is due to a change in the difference between the densities of states free for tunneling for majority and minority electrons in the case of varying voltage sign and value. This result greatly differs from Slonczewski theory for the spin efficiency (3) of spin-transfer torque, where it is independent of the applied voltage. In view of this, it is important to establish the effect of strong asymmetry of the voltage dependence of the torque on spin-state instability threshold currents calculated within the framework of Slonczewski theory and the theory taking into account a change in the spin-efficiency coefficients upon voltage variation.

ANALYSIS OF THE SPIN-STATE STABILITY OF THE UNFIXED (FREE) MAGNETIC LAYER

We analyze the equilibrium spin state of the free layer by studying the evolution of its magnetization $\mathbf{m}$ in the macrospin approximation near critical points of the initial dynamic system, where we can use linearization of the matrix system of equations (1) describing this system in terms of projections onto the x, y, and z axes. We perform the calculation for the in-plane geometry of the free magnetization of a vacuum magnetic tunnel structure.

For the chosen magnetization geometry, we assume the vector of polarization of the layer with

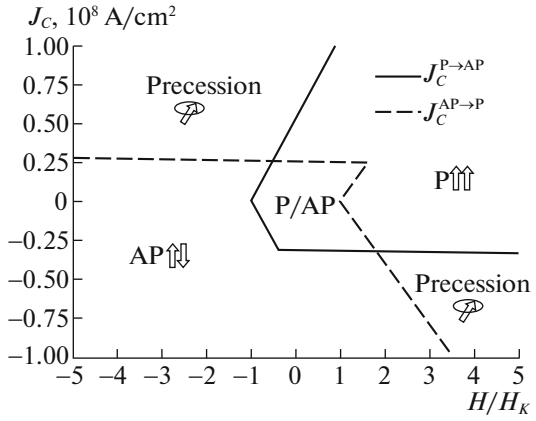

Fig. 3. Current–field phase diagram of magnetic states of the free layer for in-plane geometry of the vacuum tunnel structure without regard for the voltage dependence of the spin torque. P and AP are regions of parallel and antiparallel states, respectively and P/AP is the hysteresis region.

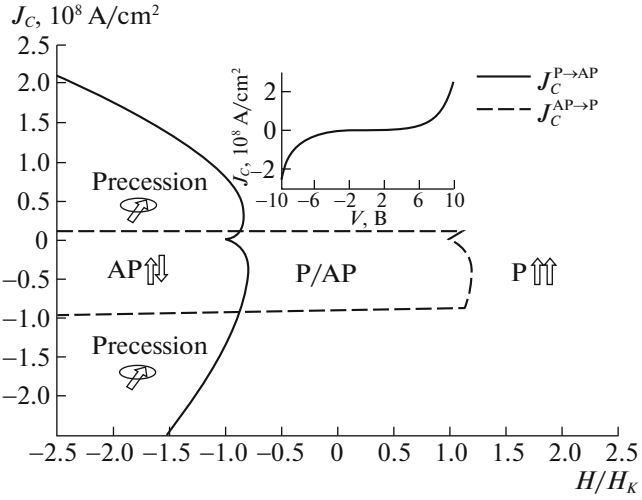

Fig. 4. Current–field phase diagram of magnetic states of the free layer for the in-plane geometry of magnetization of the vacuum tunnel structure with regard to the voltage dependence of the spin torque. The insert shows the I–V characteristic of the vacuum tunnel structure.

fixed magnetization $\mathbf{m}_P$ to be directed along the OX axis and the magnetization $\mathbf{m}$ of the free layer to be initially collinear to the vector $\mathbf{m}_P$ and directed along the easy axis of the in-plane magnetic anisotropy. In this case, the resulting effective field is written in the form

$$\mathbf{H}^*_{EFF} = \left(H_K m_X + H + H^T_{EFF\perp X}\right)\cdot \mathbf{e}_X + \mathbf{H}^T_{EFF\|Y}\cdot \mathbf{e}_Y + \left(H^T_{EFF\|Z} - H_D m_Z\right)\cdot \mathbf{e}_Z,$$

where $H^T_{EFF\|Y} = H^J_S \eta_\| m_Z$; $H^T_{EFF\|Z} = -H^J_S \eta_\| m_Y$; $H^T_{EFF\perp X} = H^J_S \eta_\perp$; $H^J_S = \dfrac{1}{\mu_0 M_S d_F}\dfrac{\hbar J}{2e}$.

It follows from Eq. (1) that the equilibrium state $\mathbf{m}^0 = (\pm 1, 0, 0)$ of the free layer is its stationary point. After linearization of system (1) with respect to the small deviations $\{\delta m_Y, \delta m_Z\}$, we obtain a characteristic equation. Analysis of its roots allows us to establish the type of approaching equilibrium for the trajectory of the magnetization motion. The threshold current densities of equilibrium state switching can be determined from the condition of the occurrence of the negative real part of these roots. The calculation will yield the next formulas for the threshold current densities needed to switch the parallel and antiparallel equilibrium states

$$J_C^{P\to AP} = -\frac{2e\alpha\mu_0 M_S d_F\left(H + H_K + \dfrac{H_D}{2}\right)}{\hbar\left(\eta_\|^P + \alpha\eta_\perp^P\right)}, \quad (4)$$

$$J_C^{AP\to P} = \frac{2e\alpha\mu_0 M_S d_F\left(-H + H_K + \dfrac{H_D}{2}\right)}{\hbar\left(\eta_\|^{AP} + \alpha\eta_\perp^{AP}\right)}, \quad (5)$$

where $\left\{\eta_\|^P, \eta_\perp^P\right\}$ are the spin-efficiency components for the parallel (P) equilibrium state and $\eta_\|^{AP}$ *and* $\eta_\perp^{AP}$ are the spin-efficiency components for the antiparallel (AP) equilibrium state.

In contrast to the expressions obtained in [11], formulas (4) and (5) take into account the contribution of the perpendicular spin-torque component to the general magnetodynamics of the free layer.

According to the described analysis of stable spin states, it follows from the calculation that at a fixed spin polarization of $P = 0.35$ [12] typical for the cobalt electrodes, the phase diagram determining regions of instability of equilibrium configurations of the magnetization of the tunnel structure on the current–field parameter plane in the framework of the Slonczewski model of spin-transfer torques is determined by the fixed parameters of the spin efficiency (3) and has the form presented in Fig. 3. The calculated parameters are $\alpha = 0.01$, $\mu_0 M_S = 1.79T$, $d_F = 2.5$ nm, $H_K = 150$ Oe, $H_D = M_S$, $P = 0.35$, and $\beta = 1$.

The calculated diagram of macrospin states on the current–field parameter plane in the presence of voltage dependences of the spin-torque components $T_\|(V)$ and $T_\perp(V)$ (Fig. 2) is shown in Fig. 4 for the calculated parameters used in the previous model. The I–V characteristic of the investigated vacuum tunnel structure is shown in the insert in Fig. 4.

The obtained diagram is significantly different from the diagram for constant torques. At low voltages, the phase diagram repeats the behavior of a diagram calculated from analytical expressions for coefficients $\eta_\|$ and $\eta_\perp$ corresponding to the Slonczewski

theory [9]. The perpendicular spin-torque component greatly affects the kink of side lines limiting the hysteresis region (P/AP). The specific features of the calculated voltage dependences of the spin-torque components are the most pronounced in the phase diagram at voltages close to the field-emission mode. In particular, the threshold line $J_C^{P\to AP}$ has an inflection toward negative external magnetic fields. This is due to rapid growth of the parallel spin-torque component $T_\parallel$ under positive voltages and variation in the sign of both torque components under negative voltages. The threshold line $J_C^{AP\to P}$ is characterized by a weak effect of the perpendicular torque component $T_\perp$ on the characteristics of the transition in the weak-field region, while in the range $H \geq H_K$, where H_K is the magnetic anisotropy field, one can observe a significant change in the critical line that determines the threshold values related to the external-magnetic-field variation.

Thus, in the vacuum tunnel structure high voltage asymmetry of the spin-transfer torque is observed, which is caused by different changes in the density of levels free for tunneling in the second order of voltage upon voltage-sign variation. As was shown in [13], this effect is related to asymmetry of the spin polarization of current. This asymmetry is retained in the vacuum structure. Here, as in tunnel structures with a dielectric barrier, an important role in switching the magnetic state of the free layer can be played by the fairly large transverse torque component.

The calculated features of the voltage dependences of the spin-torque components for field-emissionon magnetic structures allow us to state that, in contrast to tunnel structures with a dielectric spacer, the hysteresis of magnetic-state switching cannot be observed at a fixed magnetic field and varied field-emission current, at least for the considered parameters of the free magnetic layer. Upon a variation in the field-emission current, only the transition from the static magnetization state to spin precession can occur.

The results obtained can be used in the spin-polarized microscopy study of spin-transfer torques in vacuum tunnel structures and in the development of new devices based on current transfer of the spin in nanoscale tunneling heterostructures.

ACKNOWLEDGMENTS

This study was supported by the Russian Foundation for Basic Research, project no. 13-07-12405, and by the Ministry of Education and Science of the Russian Federation, project no. 14.578.21.0001 (id RFMEFI57814X0001).

REFERENCES

1. T. Shinjo, *Nanomagnetism and Spintronics*, 1st ed. (Elsevier Science, UK, 2009), p. 1.
2. K. A. Zvezdin, M. Yu. Chinenkov, A. F. Popkov, et al., Inzh. Fiz., No. 10, 27 (2012).
3. A. F. Popkov, K. A. Zvezdin, M. Yu. Chinenkov, et al., Inzh. Fiz., No. 9, 19 (2012).
4. A. Manchon, S. Zhang, and K.-J. Lee, Phys. Rev. B. **82**, 174420 (2010).
5. J. Zhang and R. M. White, J. Appl. Phys. **83**, 6512 (1998).
6. G. Herzog, S. Krause, and R. Wiesendanger, Appl. Phys. Lett. **96**, 102505 (2010).
7. H. F. Ding, W. Wulfhekel, J. Henk, et al., Phys. Rev. Lett. **90**, 116603 (2003).
8. H. Xi, J. Stricklin, H. Li, Y. Chen, et al., IEEE Trans. Magn. **46**, 860 (2010).
9. J. Slonczewski, Phys. Rev. B **71**, 024411 (2005).
10. P. Ogrodnik, M. Wilczyński, R. Świrkowicz, and J. Barnaś, Phys. Rev. B **82**, 134412 (2010).
11. J. Grollier, V. Cros, H. Jaffris, et al., Phys. Rev. B **67**, 174402 (2003).
12. J. Mathon and A. Umerski, *Physics of Low Dimensional Systems*, Ed. by J. L. Morán-López (Springer US, USA, 2001), p. 363.
13. D. Datta, B. Behin-Aein, S. Datta, and S. Salahuddin, IEEE Trans. Nanotech. **11**, 261 (2012).

Translated by E. Bondareva